AD NUMBER

AD449522

LIMITATION CHANGES

TO:

Approved for public release; distribution is unlimited.

FROM:

**Distribution authorized to U.S. Gov't. agencies and their contractors;
Administrative/Operational Use; AUG 1964. Other requests shall be referred to Office of Naval Research Laboratory, Washington, DC 20360.**

AUTHORITY

onr ltr 5 jul 1966

449522

Contract NONR 3437(00)

Semiannual Technical Summary Report

Period Ending 19 August 1964

"STABLE DENSE COLD PLASMA"

Advanced Research Projects Agency
Order No. 194, Amendment No. 5
Program Code No. 4980
Contract Date 20 February 1961, Completion 19 February 1965
Issued in Amount of $507,995, as Amended

Project Scientist: Dr. S. Naiditch

UNIFIED SCIENCE ASSOCIATES, INC.
826 south arroyo parkway
pasadena, california
murray 1-3486

ABSTRACT

The major efforts in the past quarter have been directed toward (1) validating our electrodeless Hall measurement technique, (2) measuring densities of liquid sodium ammonia solutions from -60 to +60°C, (3) studying the conductivities of $Na-NH_3$ solutions, and (4) improving our solution preparation techniques to enable us to increase lifetimes at elevated temperatures or attainment of higher temperatures.

SECTION I - HALL EFFECT MEASUREMENTS

I.1 ABSTRACT

The experimental apparatus for electrodeless determinations of Hall coefficients of fluids has been assembled, except for the temeperature environmental chamber, and tested with a standard solid state semi-conducting Hall cell. The results on the standard Hall cell have been excellent and indicate that the apparatus has the capability of measuring the Hall coefficient of solutions with electron concentrations down to 10^{-19} with an accuracy of better than 2 percent; or, in terms of the usual criterion in assessing the performance of a Hall circuit, a detectability of a Hall mobility, $R_h \times \sigma$, of 10^{-2} cm^2 V^{-1} sec^{-1}.

I.2 INTRODUCTION

The Hall effect is the phenomenon that occurs when a current carrying conductor is placed in a transverse magnetic field. The interaction of electric current and magnetic field B produces an electric field which is perpendicular to both B and the direction of the current density j. The Hall field E_h is described by the equation

$$E_h = R_h \cdot j \cdot B \qquad (1)$$

R_h is a proportionality constant called the Hall coefficient. The density and nature of the charge carrier may be deduced from this coefficient. A better understanding of the mechanism of electrical conductivity in sodium ammonia solutions can therefore be expected from these measurements.

For the precise determination of Hall coefficients, the usual method is to measure the d.c. Hall voltage. In the case of very small Hall coefficients, the results of d.c. measurement can be obscured by a number of effects.

Misalignment of the probes for detecting the Hall voltage results in an unbalanced potential difference V_s, due to the probes not being on an equipotential. In an earlier progress report[1], the following equation was derived for the ratio r of unbalanced voltage V_s, to Hall voltage V_h.

$$r = \frac{V_s}{V_h} = \frac{4.f}{\sigma \cdot R_h B} \qquad (2)$$

where f is the fractional misalignment of the two probes compared to the length of the specimen and σ is the conductivity of the specimen. If a magnetic field of 10^4 gauss is assumed, typical values for σ and R_h which are based on an electron density of 10^{19} yield the relation

$$r = 7 \times 10^4 f. \qquad (3)$$

From equation (3) it is seen that it is mechanically impossible to reduce the alignment error of a glass blown system to such a small value as to make the ratio r equal to one.

Additional distortion of d.c. measurements are caused by Ettinghausen, Nernst, Reghi-Leduc and thermoelectric effects. Because of the long time required by these effects, distortions of Hall voltage measurements can be avoided if an a.c. specimen current is used instead of d.c. current.

The errors caused by probe misalignment can be eliminated if a double a.c. method is applied. In this technique, both an a.c. specimen current and an a.c. magnetic field are used. The primary specimen current is applied at one frequency and the magnetic field at another. From equation (1), one can see that a Hall voltage of two beat frequencies is produced which can be filtered out from the unbalanced voltage V_s, due to alignment errors.

Detecting the amplitude of one frequency component of the Hall voltage yields the coefficient R_h. The advantage of the double a.c. method is the generation of a Hall voltage at a frequency different from that of all other signals. The frequency separation permits application of highly selective filters in conjunction with narrow band amplification to detect even a very small Hall voltage in the presence of a high noise level. The high sensitivity makes the double a.c. method applicable to the determination of Hall coefficients of substances with high electron densities.

In the present case of a sodium ammonia solution, additional difficulties arise from the chemical properties of the substance. The catalytic effects of any metal used as an electrode preclude placing electrodes in contact with the plasma. For this reason, an electrodeless method has been developed to measure the Hall coefficient of sodium ammonia solutions.

1.3 THE EXPERIMENTAL METHOD

The problem of eliminating the electrodes in contact with the specimen has been solved by using an inductive method for generating the a.c. specimen current and measuring the Hall voltage. The specimen is contained in a closed loop circuit which is inductively coupled to a signal source. A flat, rectangular section of the loop is placed in an a.c. magnetic field B which is perpendicular to the specimen current in this section. The method is schematically indicated in figure 1. The specimen current I is induced in coil 1 of transformer 1. The primary coil of transformer 1 is driven by a signal generator and a subsequent amplifier. In order to utilize the high sensitivity of the double a.c. method, a frequency of 460 cps has been chosen for the specimen current and a 60 cps a.c. magnetic field is applied to the flat section of the specimen. The frequency of the magnetic field has been chosen to supply economically the necessary power for the magnet.

The specimen current I is measured with the aid of transformer 2. Coil 2 of this transformer is included in the loop of the specimen current. For a fixed load resistor, the output voltage of transformer 2 is a unique function of I. Calibration of transformer 2 permits quantitative measurements of the specimen current.

The Hall field E_h is generated perpendicular to both the current I and the magnetic field B. For measuring the Hall voltage, a closed transverse loop of the specimen is attached to the rectangular section which is placed in the a.c. magnetic field. The joints 3 and 4 in figure 1 are oriented perpendicular to I and B. The Hall field produces a Hall voltage between 3 and 4 at the beat frequencies 400 cps and 520 cps, the 400 cycle component of the Hall voltage being measured. A Hall current produced by the Hall field is detected with the aid of transformer 3. Transformer 4 is used to induce a 400 cycle compensation voltage in coil 4 which is included in the transverse loop of the specimen. The compensation voltage is generated in opposite phase to the Hall voltage. A voltage divider controls the input voltage of transformer 4. The induced compensation voltage which nulls the Hall current equals the Hall voltage in magnitude. Measuring this voltage is equivalent to measuring the Hall voltage. The open circuit voltage across coil 4 is a unique function of the input current of transformer 4. Calibrating transformer 4 by measuring the open circuit output voltage versus input current permits quantitative measurements of the Hall voltage. The input current is measured by monitoring the voltage drop across a viewing resistor.

The 400 cycle compensation voltage is derived from the same signal sources which generate the Hall voltage. A 460 cps alternating current passes through a solid state Hall cell in a 60 cycle magnetic field. The 400 cycle

component of the output voltage is used as the compensation voltage. This way of generating the compensation voltage enables us to measure the sign of the Hall effect in the specimen under investigation by comparing the phase of the Hall voltage with the phase of the signal generated by the known solid state Hall cell. The sign of the Hall effect is important for determining the nature of the charge carrier in the specimen.

The liquid specimen is contained in a glass cell which includes a flat rectangular section, the specimen current loop with the coils 1 and 2, and the transverse loop with the coils 3 and 4. A picture of the assembled glass cell is shown in figure 2. The loop circuits are designed to fit the magnet.

The a.c. magnetic field B is measured by means of a flux sensing coil which is located in the field adjacent to the rectangular section of the specimen.

The signals which are obtained from the transformers 2, 3, 4 and the flux sensing coil pass a filter circuit before they are measured with a lock-in amplifier. A diagram of the filter circuit is shown in figure 3. The output voltage of the Hall current detection transformer 3 is the smallest signal which has to be detected. In order to reduce 460 and 60 cycle pickup noise, bucking coils are inserted in the input lead of this signal. A rotary switch connects the incoming signals with the lock-in amplifier, which is a tunable, narrow band device with a phase sensitive detector. The detector requires a reference voltage for each signal. The necessary circuits for generating reference voltages are included in the diagram of the filter circuit. The Hall generator which produces the 400 cycle compensation voltage is also part of the same circuit.

The transformers for measuring specimen current and Hall voltage are mounted relatively close to the a.c. magnet. In order to reduce 60 cycle pickup noise, all transformers are enclosed by aluminum shields. The thickness of the shields is equal to the skin depth corresponding to 60 cycle a.c. currents.

The Hall voltage which is generated at the free ends of a sample is reduced by end effects[2][3]. The correction factor $F(\frac{L}{W})$ is a function of the ratio of length L to width W. If the ratio is infinite, $F(\frac{L}{W})$ becomes unity. For

$$\frac{L}{W} = 4,$$

the correction factor is

$$F(4) = 0.997.$$

The assembled Hall cell is designed for a length-to-width ratio equal to four to make the deviation of $F(\frac{L}{W})$ from unity small.

1.4 TEST OF THE APPARATUS BY MEASURING HALL EFFECT OF A SOLID STATE CELL

The experimental apparatus to determine the Hall coefficients of fluids has been assembled, except for the temperature environmental chamber. In a preliminary experiment, the function of the setup was tested with a standard solid state Hall cell. During this experiment, the Hall voltage was measured by determining the Hall current. This method was used for the reason of simplifying the measurement. The error which is caused by this method is relatively small.

Transformers 2 and 4 were calibrated for the measurement of specimen and Hall current by determining the output voltage as a function of input

current at the corresponding frequencies. Insertion losses of the filter circuit were included in the calibration. The output voltages were measured with the lock-in amplifier. Calibration curves of the detection transformers are shown in figures 4 and 5.

The Hall current was measured for different values of magnetic field and fixed specimen current. The 60 cycle magnetic field was determined by measuring the output voltage of the flux sensing coil with the lock-in amplifier. The measured Hall current versus reading of the lock-in amplifier is plotted in figure 6. The reading of the lock-in amplifier is proportional to the output voltage of the flux sensing coil and to the applied magnetic field. The measurements are very close to a straight line according to the proportionality between Hall voltage and magnetic field.

1.5 CONCLUSIONS

The measurements on the solid state Hall cell proved that the selectivity of the filter circuit and the lock-in amplifier is sufficiently high to reduce pickup noise to a negligible level. From the observed noise level and the available amplification, one can conclude that the assembled apparatus has the capability of measuring Hall coefficient of cold plasmas with electron concentrations up to 10^{19} with an accuracy of 2 percent or, in terms of the usual criterion in assessing the performance of a Hall circuit, a detectability of a Hall mobility $R_h \cdot \sigma = 10^{-2}\ cm^2\ V^{-1}\ sec^{-1}$.

SECTION 2 - DENSITIES

The height of the meniscus of a solution in a tube relative to a fiducial mark is measured with a cathetometer. The volume of the sample is determined from the values of the cross-sectional area of the tube and the volume at the fiducial mark. Sample composition is determined from conductivity measurements at -33.5°C. Densities are then calculated from the volume-temperature results using Kraus'[5][6] densities at -33.8°C as a reference. Vapor pressure corrections are applied using estimates of the ratios of the vapor pressures of the solutions to those of ammonia, obtained from the literature[7][8]. This ratio is assumed to remain approximately constant at all temperatures and to vary only with composition. This assumption is adequate within the accuracy of our measurements.

2.1 EXPERIMENTAL

The experimental system is designed to determine both the density and conductivity of a sample over a wide range of temperatures.

The sample is situated in an oven whose temperature is controlled and may be raised or lowered with heating coils or bursts of liquid CO_2. The temperature in the oven is controlled by a Fenwall differential expansion bi-metal controller which can be set to control at temperatures between -80° and +200°C. Constant temperature is maintained by actuation of a solenoid controlled liquid CO_2 injection system at low temperatures, or the current through nichrome wire heating coils at high temperatures. A fan circulates the atmosphere inside the oven and baffles serve to provide uniform flow across the sample. The sample is viewed through pyrex glass windows coated with an infrared reflecting film. A fluorescent lamp placed outside the oven at the far side window serves to illuminate the meniscus.

The meniscus is viewed through a 90° prism in order to keep both cathetometer and operator out of the direct line of sight if rupture of a sample tube occurs. The oven is provided with an electrodeless conductivity device used to determine conductivities at each temperature.

The accuracy of the system has been established using sample tubes containing mercury at temperatures between +20 and 120°C, and liquid ammonia from -60 to +60°C. The experimental errors in density for pure liquid ammonia amounted to ± 0.3 percent at the higher temperatures. The experimental error in the densities of the sodium ammonia solutions is estimated to be about ± 0.5 percent. This error may be larger for temperatures above +40°C.

2.2 SAMPLE PREPARATION

Sodium solutions of high temperature stability were prepared as described previously in these reports. Both volumes and conductivities can be measured at various temperatures. The reproducibility of the volumes and conductivities can be checked for decomposition on returning to low temperatures. This check was performed only on about 5 percent of the samples since most of the samples ruptured at between 55 and 62°C. However, the stability of samples has been established for temperatures up to 150°C in our earlier experiments.

2.3 SAMPLE CONTAINERS

The solutions are sealed in pyrex glass sample tubes, with a toroid at one end. The toroidal section is used to determine electrical conductivities by the electrodeless inductive method. Decal fiducial marks are baked onto the straight portion of the sample tubes approximately five inches apart. The volumes at the fiducial marks are determined volumetrically with mercury.

2.4 EXPERIMENTAL RESULTS

Densities have been determined for sodium ammonia solutions at temperatures between -60 and +60°C. Volumes and electrical conductances are measured simultaneously. The results of the measurements are shown in figure 7 where densities are plotted as a function of mole fraction for various temperatures.

The variation of the apparent molal volume V_{Na} (i.e., the volume of solution minus the volume of ammonia per mole of sodium) at mole fractions of 0.03 and 0.07, with temperature are plotted in figure 8. These results show that the apparent molal volume decreases as the temperature of the solution is increased.

The experimental activation energy ΔE has been calculated for each run from Arnhenius plots of logs of densities versus reciprocals of temperatures. Values of ΔE at -40, 0, +40°C have been plotted against mole fraction in figure 9. These values are shown to increase with temperature and decrease with concentration.

SECTION 3 - CONDUCTIVITIES

Additional measurements of the high temperature conductivities of sodium-ammonia solutions have been made along the vapor pressure curves. Our recent data, in which the more concentrated solutions are stressed, are in good agreement with much of our earlier data. These results are shown for comparison in figures 10 and 11. For some of the more concentrated solutions, there is a sharp rise in conductivity at about 140°C. This effect will be studied further when a fast heat-cool bomb, which has been fabricated and is being installed, becomes operational.

A series of conductivity measurements at constant pressure has been initiated. Results of measurements at constant pressure are shown in figure 12. The compositions for the samples in the three figures are given in tables I and II. The effect of pressure is small for the more concentrated solutions, where it is negligible over much of the range.

At the present time, we have been unable to produce conducting gases for the more concentrated samples at temperatures up to 190°C. The use of the fast heat-cool bomb may enable us to do this by reducing the time required to reach still higher temperatures.

In the case of measurements of the effects of variation of pressure on the conductivity at constant temperature, erratic effects occur which have not yet been eliminated. To determine if the effects are caused by dissolution of nitrogen in the liquid solution, conductivity cells were prepared with long diffusion path lengths to increase the times required for dissolved pressurizing gas to reach the toroids and affect conductivities. This modification has not reduced the erratic behavior.

The pressure effect studies are of interest for several different reasons. One is that the pressure must affect hole density in the liquid which is intimately related to conductivity in dilute solutions. A second is that it has enabled us to establish that at least in the more concentrated solutions no decomposition occurs, i.e., no equilibration between sodium, ammonia, sodium ammide and hydrogen as suggested by Jolly at Lille, at least to 145°C. A third reason is that the energy of activation of conductivity at constant pressure, E_p is more easily interpreted than that along the vapor pressure curve E_{vp}.

The various conductivity measurements are related to each other as follows. If the specific conductivity, σ, is taken as a function of temperature T, pressure p, and composition, expressed here as mole fraction of sodium X_2, then

$$\sigma = \sigma (T, p, X_2),$$

and

$$d \ln \sigma = \left[\frac{\partial \ln \sigma}{\partial \frac{1}{T}}\right]_{p, X_2} d\frac{1}{T} + \left[\frac{\partial \ln \sigma}{\partial p}\right]_{T, X_2} dp + \left[\frac{\partial \ln \sigma}{\partial X_2}\right]_{T, p} dX_2$$

or, using the symbol vp to indicate measurements along the vapor pressure curve:

$$\left[\frac{\partial \ln \sigma}{\partial \frac{1}{T}}\right]_{vp} = \left[\frac{\partial \ln \sigma}{\partial \frac{1}{T}}\right]_{p, X_2} + \left[\frac{\partial \ln \sigma}{\partial \ln p}\right]_{T, X_2} \left[\frac{\partial \ln p}{\partial \frac{1}{T}}\right]_{vp} + \left[\frac{\partial \ln \sigma}{\partial X_2}\right]_{T, p} \left[\frac{\partial X_2}{\partial \frac{1}{T}}\right]_{vp}$$

Let $$\left[\frac{\partial \ln \sigma}{\partial \frac{1}{T}}\right]_{p,\, X_2} = -\frac{E_p}{R},$$

where E_p may be defined as an energy of activation. E_{vp} is defined similarly. The term

$$\left[\frac{\partial \ln p}{\partial \frac{1}{T}}\right]_{vp}$$

may be evaluated using the Clapeyron-Clausius equation

$$\left[\frac{\partial \ln p}{\partial \frac{1}{T}}\right]_{vp} = -\frac{\Delta H_{vap}}{R}$$

The magnitude of the last term

$$\left[\frac{\partial \ln \sigma}{\partial X_2}\right]_{T,\, p} \left[\frac{\partial X_2}{\partial \frac{1}{T}}\right]_{vp},$$

is generally negligible compared with the other terms.

The preceding equation may be rewritten as:

$$E_p = E_{vp} - \Delta H_{vap}\left[\frac{\partial \ln \sigma}{\partial \ln p}\right]_{T,\, X_2}$$

The preliminary experimental pressure effects appear to be in accord with this equation for concentrated solutions in which $\frac{\partial \sigma}{\partial p}$ and $E_{vp} - E_p$ are both close to zero.

SECTION 4 - SURFACE CONTAMINANTS

4.1 INTRODUCTION

The cleaning of glass surfaces to remove contaminants has been considered an art. Qualitative means, such as the ability to form breath figures, have been used as criteria. The criterion as to whether glassware is clean depends on its use. Measurements of contact angles of liquids, coefficients of friction, and adhesion of solids and films give results which are related to the physical properties of the glass surface. The method of Warshawsky[9], in which the volume of hydrogen produced by the reaction of sodium in ammonia with surface water, gives results which depend on the chemical properties of the glass surface. This technique is meaningful in our program since we are interested in increasing the high temperature stability of sodium-ammonia solutions.

4.2 EXPERIMENTAL

In the method of Warshawsky, the amount of hydrogen liberated by the reaction of a sodium ammonia solution with traces of water or other ingredients absorbed by the glass surfaces is measured. Warshawsky cleaned a tube, sealed this tube onto a vacuum system, baked the tube under vacuum, then introduced sodium by moving a small sodium covered glass bead into the sample tube by means of a magnet, after which he distilled ammonia into the tube. After allowing reaction to take place, he froze the ammonia and measured the hydrogen by use of a McLeod gage.

Our system consists of two banks, each containing ten tubes into which the sodium covered beads may be admitted. Each bank of tubes can be baked separately. The tubes are sealed into the system and the system is evacuated with or without bakeout as prescribed by the cleaning procedure.

The beads are then placed in the tubes individually and ammonia distilled in. It was found that the reaction was complete in 15 minutes at -78°C. After reaction, the ammonia is distilled into a liquid N_2 trap and the hydrogen pressure is determined with a McLeod gage.

Although the solubility of hydrogen in frozen ammonia at these pressures is negligible, it was found that as much as 96 percent of the hydrogen was trapped in the solution if it was refrozen in the original tube and the pressure measured above the frozen solution as was done by Warshawsky. We therefore distill the ammonia out of the reaction tube into a trap at liquid nitrogen temperature and allow the pressure to equilibrate.

Another approach is being considered, namely, the incorporation of the procedure described by Klingelhoefer[10]. In this method, a sodium salt dissolved in ammonia is electrolyzed, producing metallic sodium which reacts with the water in the ammonia. When the water is all reacted, the typical blue solution is produced. Klingelhoefer used this method to determine water down to 1 ppm in ammonia which is near the upper limit of the range desired. The adaptation of this method to our problem is under consideration.

4.3 RESULTS

Although water is not the only surface contaminant in glass that may lead to the evolution of hydrogen, it should be the most predominant. (We are considering -Si-OH as a form of chemisorbed water.) For this reason, we report the hydrogen given off in terms of molecules of water per square Å of glass surface. Results are given in order of increasing effectiveness of the cleaning procedure. Each result corresponds to a separate sample.

The present method provides a simple technique by which to evaluate the effectiveness of several different procedures in the cleaning of glass sample tube surfaces. The general picture of glass surfaces is that the outer layer is rather heavily eroded and contains various amounts of absorbed water. Warshawsky's results show that the major difficulty is the removal of the absorbed water. His method employs extensive bakeout under vacuum at 400°C. However, Kohl[11] states that bakeout under vacuum can never be as effective as dissolution of the outer layer with hydrofluoric acid and subsequent bakeout. Holland[12] states that bakeout at 400°C can increase the number of hydroxyl groups at the surface up to a monolayer due to diffusion from the bulk. Our results show that the sodium-ammonia solutions decomposed rapidly at -78°C when the conductivity cells were treated with HF and followed only by a water rinse and bakeout under vacuum. It appears that the effectiveness of cleaning with HF is dependent on the rinse procedure. The effectiveness is quite poor when HF is used separately with just a water rinse but it is quite good when dilute HF mixed with nitric acid and soap is used. It must be emphasized that we report larger amounts of absorbed water per square area than that indicated in Warshawsky's results. This difference might be attributed to the effect of bakeout duration.

No firm conclusions can be drawn from our results until further experiments allow us to evaluate the reliability of the data. However, it is seen that all cleaning methods leave significant quantities of water or other surface contaminants. Bakeout under vacuum reduces the amount of water in most cases and the use of HF alone as a cleaning agent appears least desirable.

SECTION 5 - WORK FOR NEXT QUARTER

A Cary Model 14 Recording Spectrophotometer has been ordered and is scheduled for arrival in early September. A heavy-walled quartz spectral cell suitable for high pressures has been designed for use with this instrument. Data in the literature give very little information on the temperature dependence of the absorption spectra for sodium-ammonia solutions and none at all at the elevated temperatures presently being used in the cold plasma conductivity studies.

This instrument will be equipped for reflectance measurements which will enable us to correct the absorption data for reflection peaks. It is planned to use fast scans at a number of temperatures. In addition, we plan to see whether it is a good analytical tool for measuring low concentrations of dissolved silicates and decomposition products such as sodium amide. This may enable us to detect materials which do not affect the conductivity but which could catalyze the decomposition of the sodium-ammonia solution.

Two problems have previously prevented the determination of absorption spectra for these solutions at high temperatures. The first, that of relatively poor stability at high temperatures, has been shown to be at least partially overcome by the stability of the samples used for high temperature conductivity determinations in this laboratory. It is hoped that stability may be further increased by the application of results of the present studies for determining surface contaminants which affect stability. The second, that of extremely high vapor pressures of the solutions at high temperatures, may be overcome by the use of the high pressure spectral cell previously mentioned.

Next quarter, we plan to complete Hall effect measurements on mercury, then to initiate studies on sodium-ammonia solutions. Initially, the samples will be run from room temperature to -80°C. Density and conductivity measurements will be continued with the extension of densities to higher temperatures using heavy-walled tubing for the density cells. A stainless steel bomb has been constructed and will be incorporated into the gas analysis system. This bomb will allow both total weight and composition determinations to be carried out on the solutions.

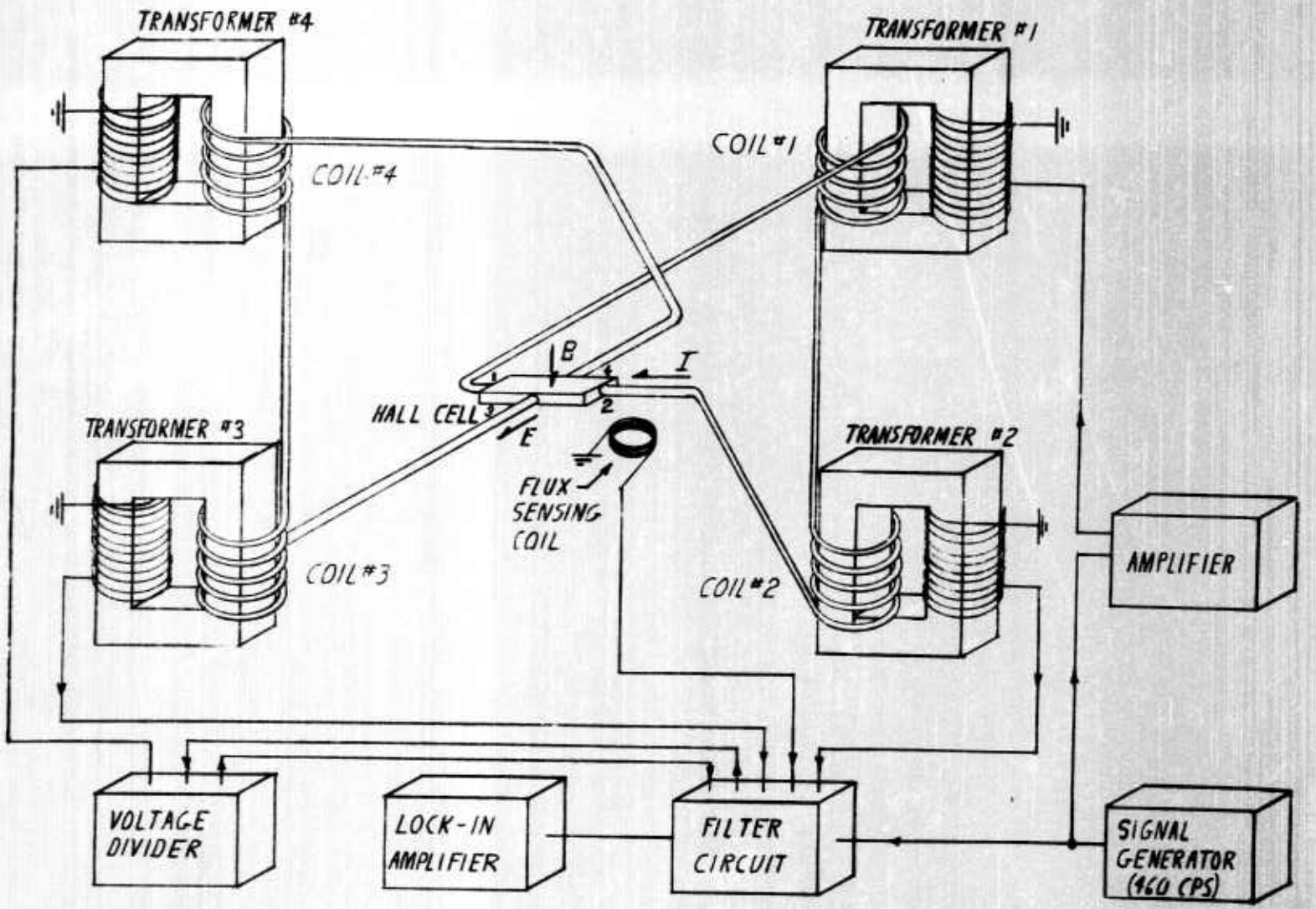

HALL CELL AND BLOCK DIAGRAM OF DETECTION CIRCUIT

FIGURE 1

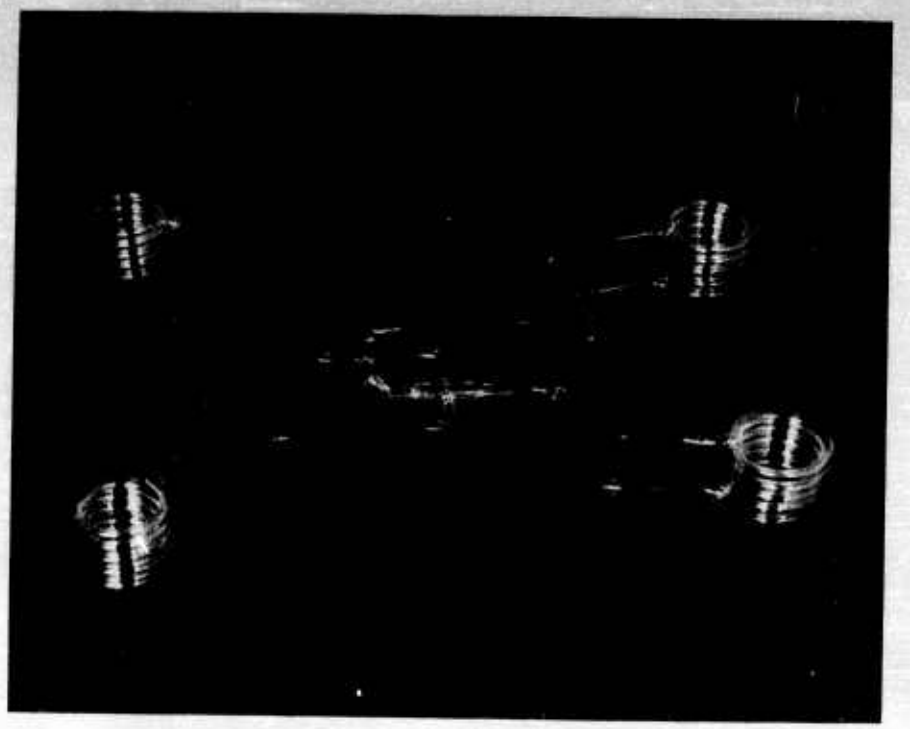

HALL CELL WITH GLASS COILS FOR INDUCING THE
EXCITER CURRENT IN THE SAMPLE MATERIAL
AND DETECTION OF HALL VOLTAGE

FIGURE 2

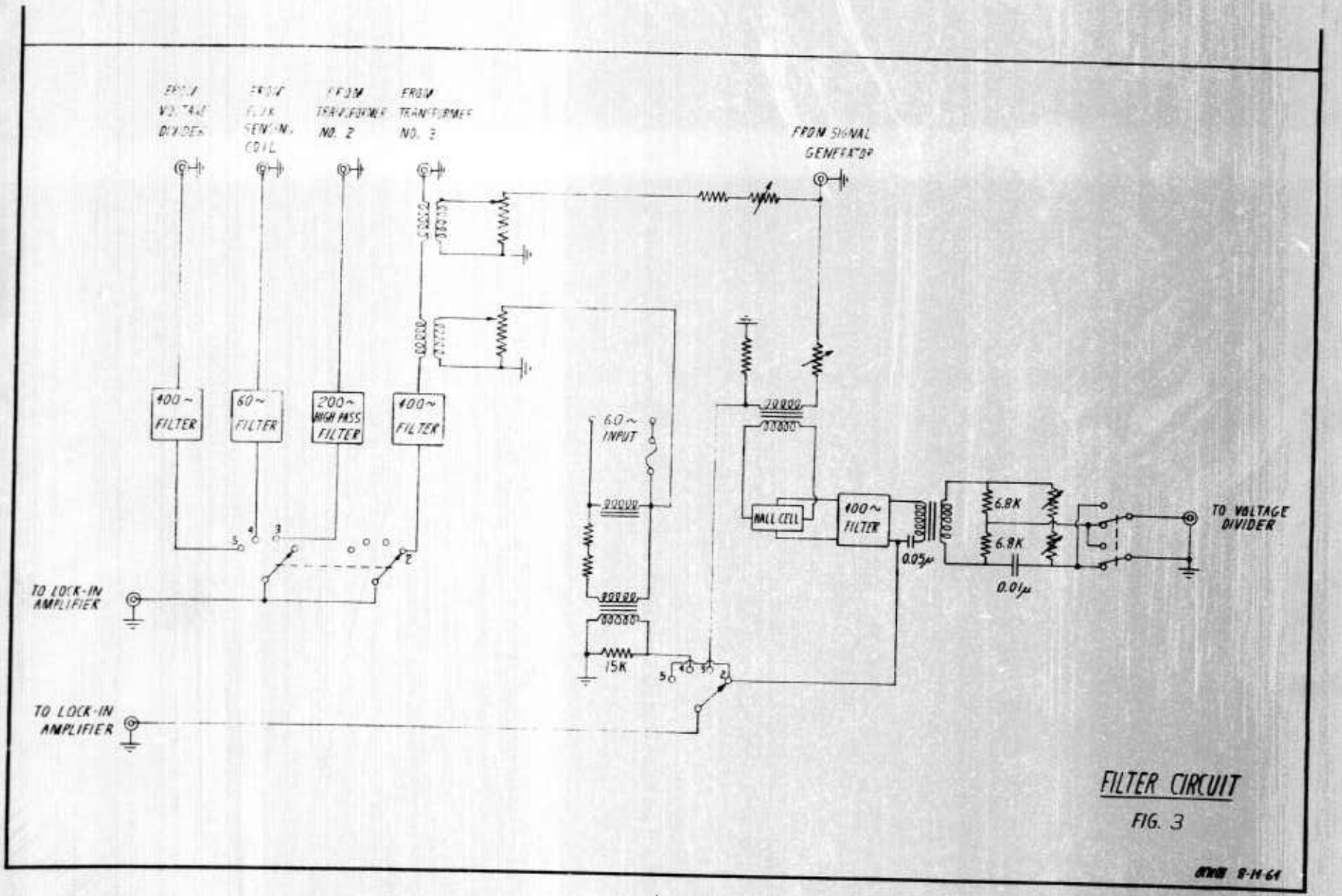

FILTER CIRCUIT

FIG. 3

8-14-64

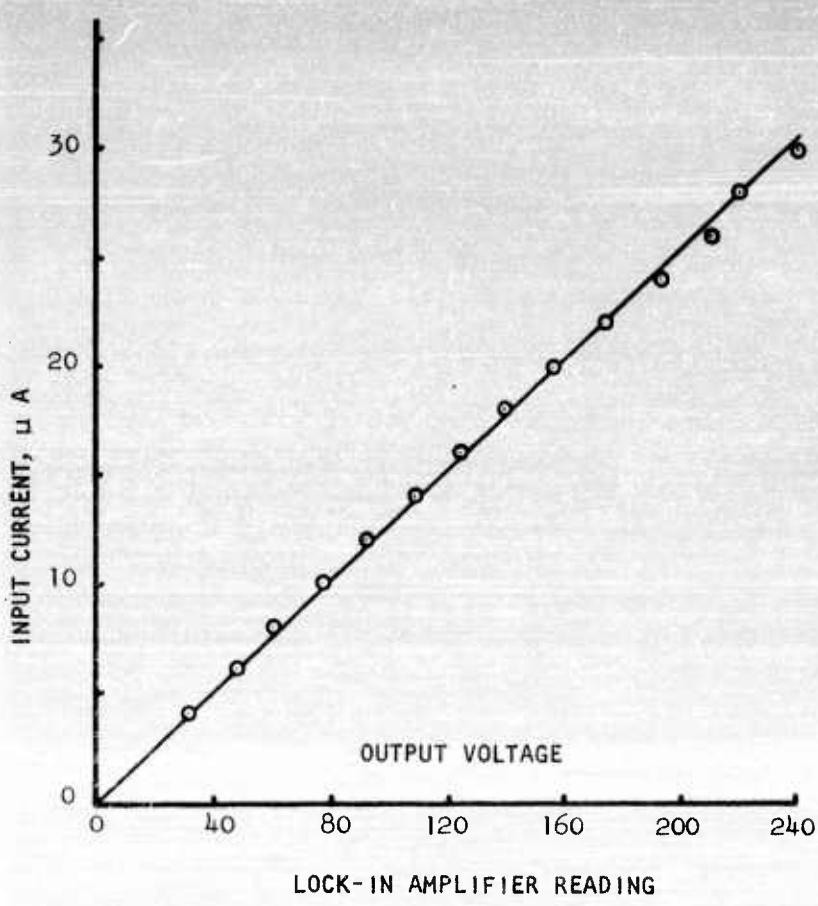

FIGURE 4: CALIBRATION OF HALL CURRENT DETECTION TRANSFORMER

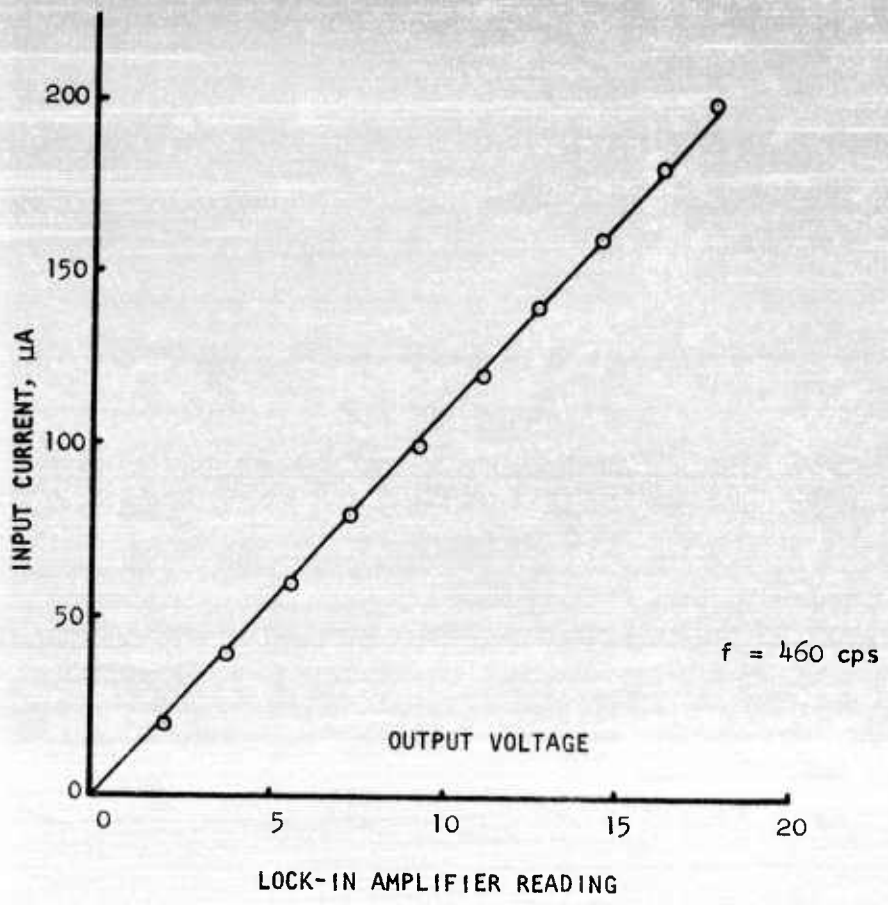

FIGURE 5: CALIBRATION OF EXCITER CURRENT DETECTION TRANSFORMER

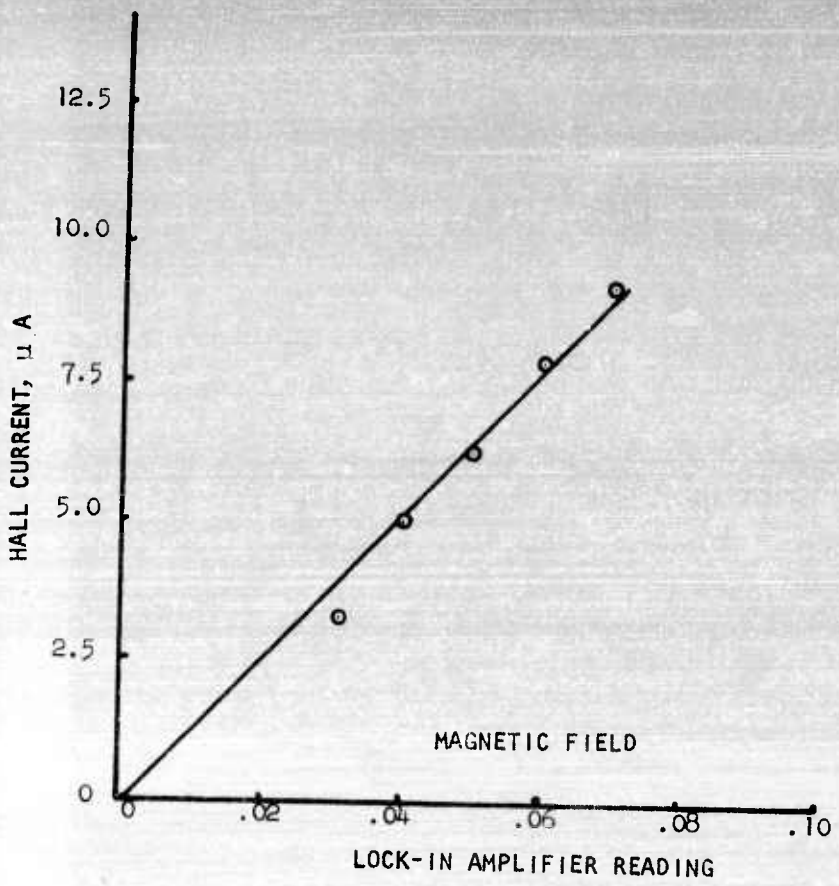

FIGURE 6: HALL CURRENT vs MAGNETIC FIELD

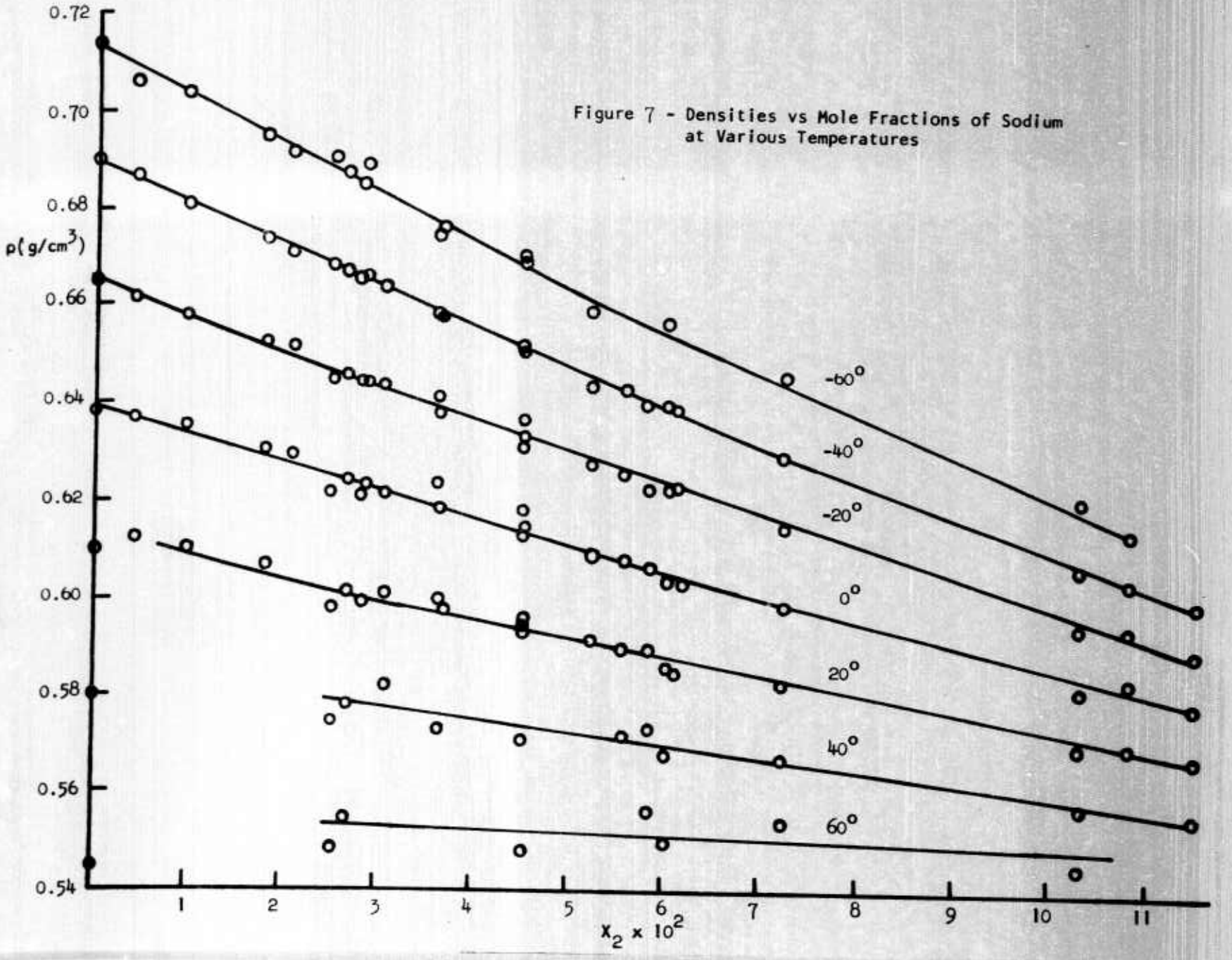

Figure 7 - Densities vs Mole Fractions of Sodium at Various Temperatures

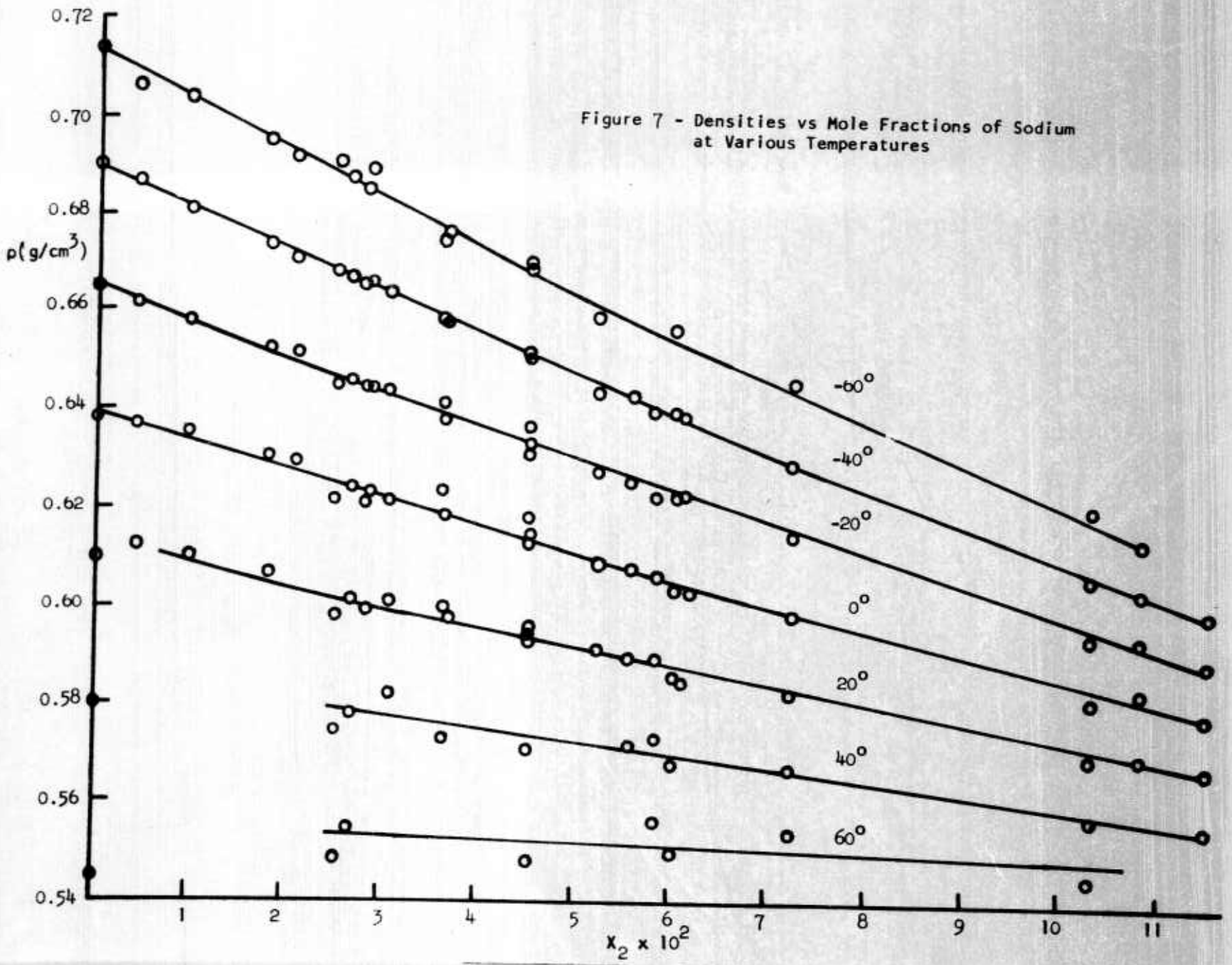

Figure 7 - Densities vs Mole Fractions of Sodium at Various Temperatures

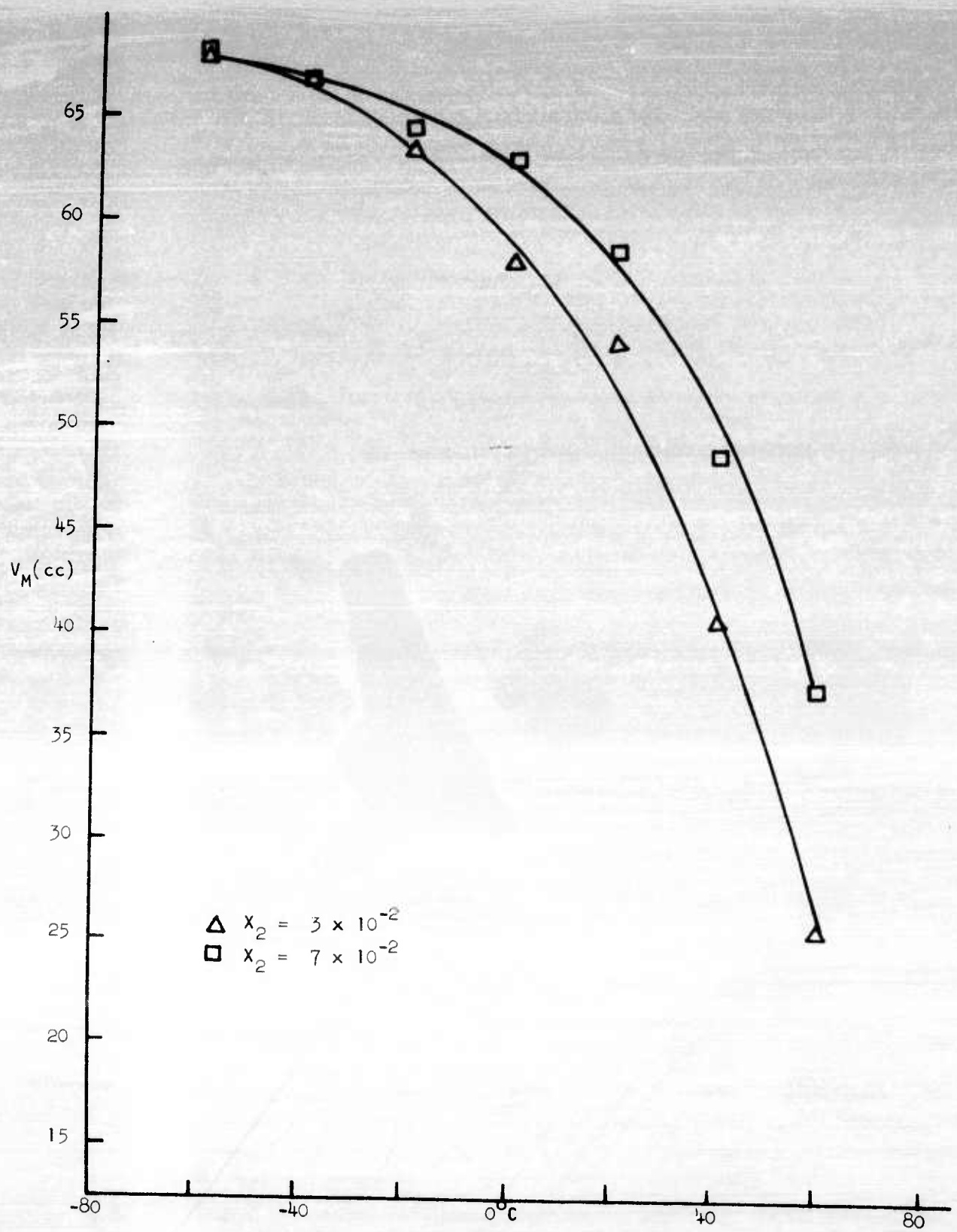

Figure 8 - Apparent Molal Volume vs Temperature for Two Compositions

Figure 9 - Experimental Activation Energy vs Mole Fraction of Sodium at +40, 0, and -40°C

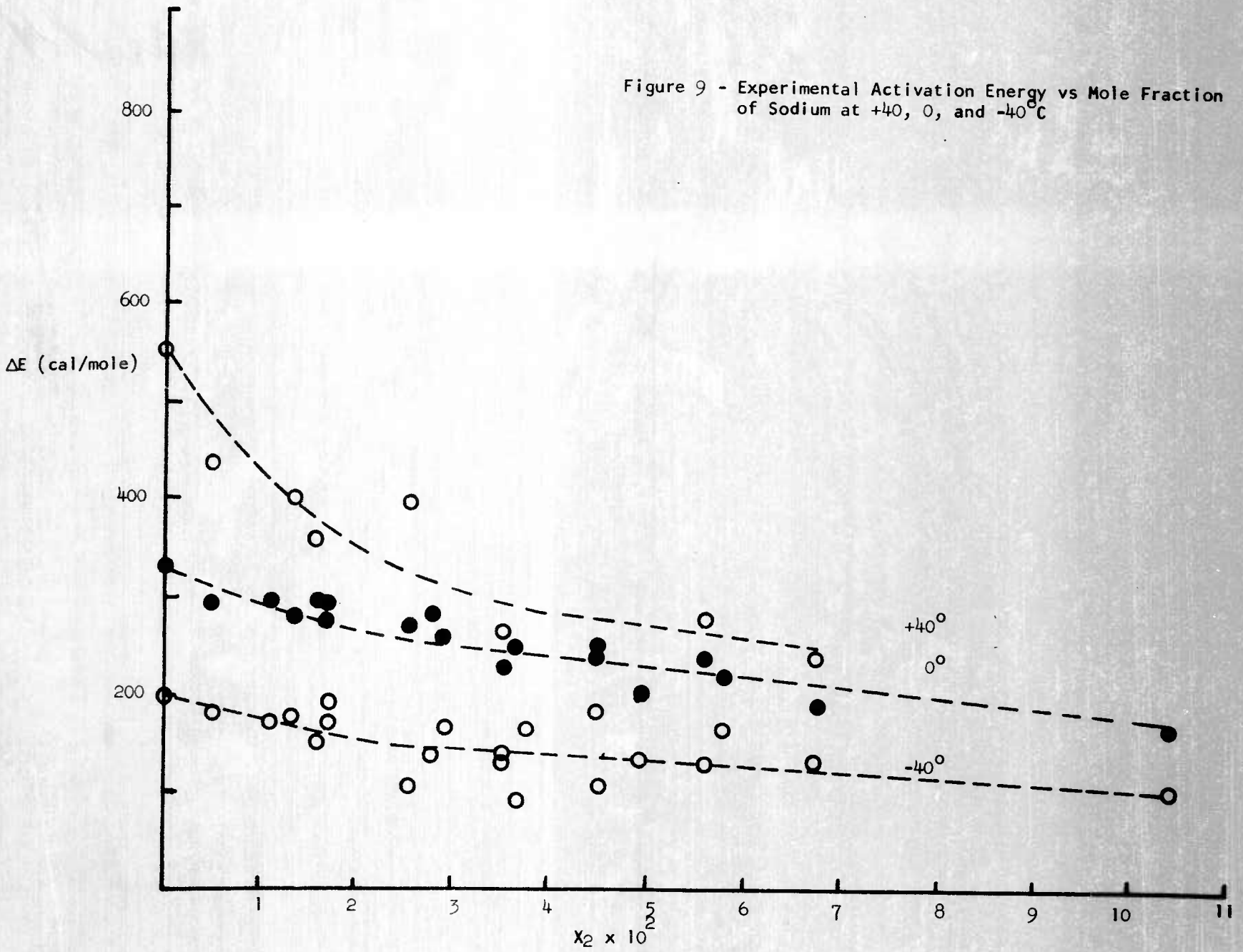

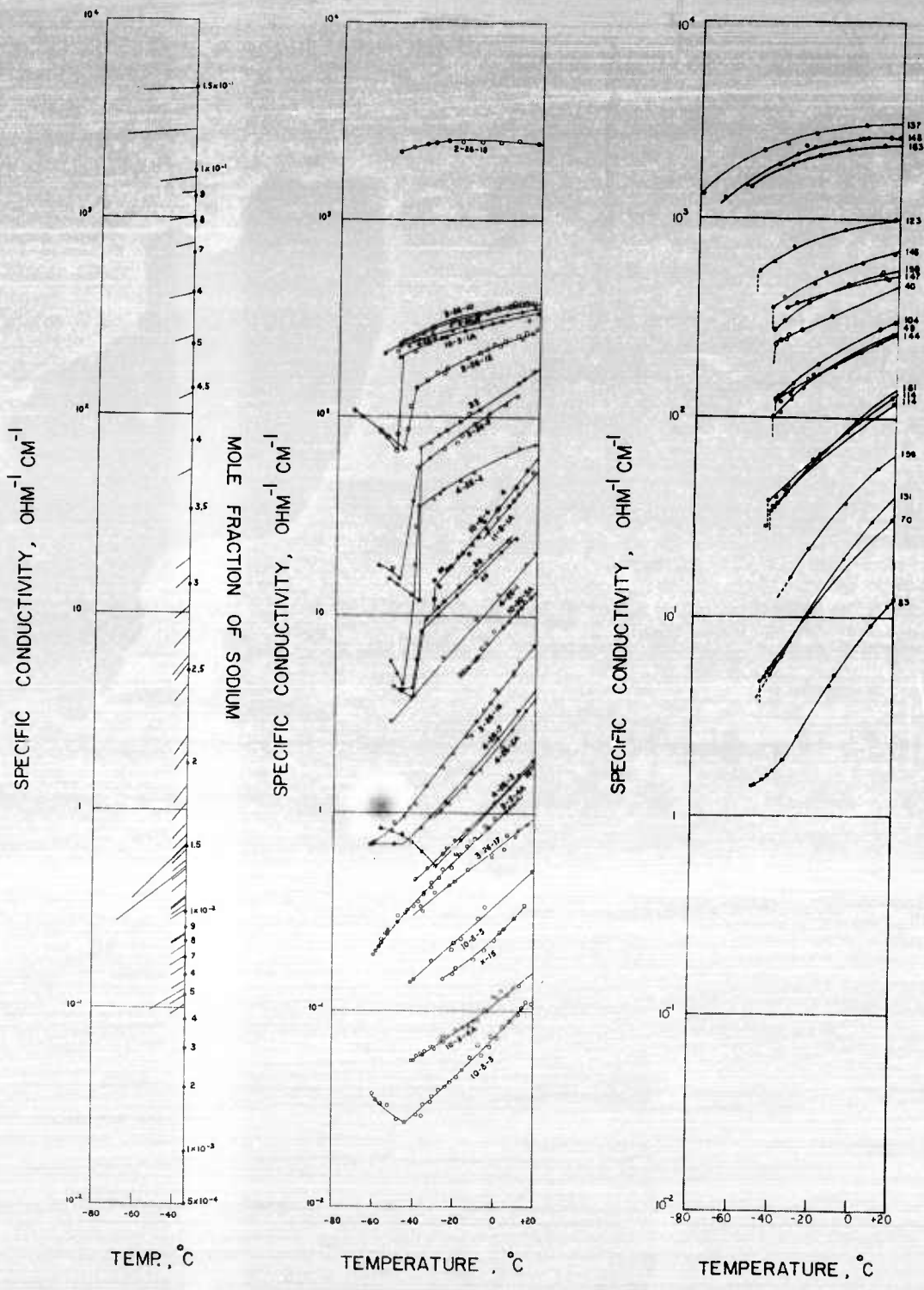

FIGURE 10-ELECTRICAL CONDUCTIVITY-TEMPERATURE DATA BELOW ROOM TEMPERATURE

KRAUS', EARLIER, AND RECENT DATA ARE DISPLAYED RESPECTIVELY FROM LEFT TO RIGHT.

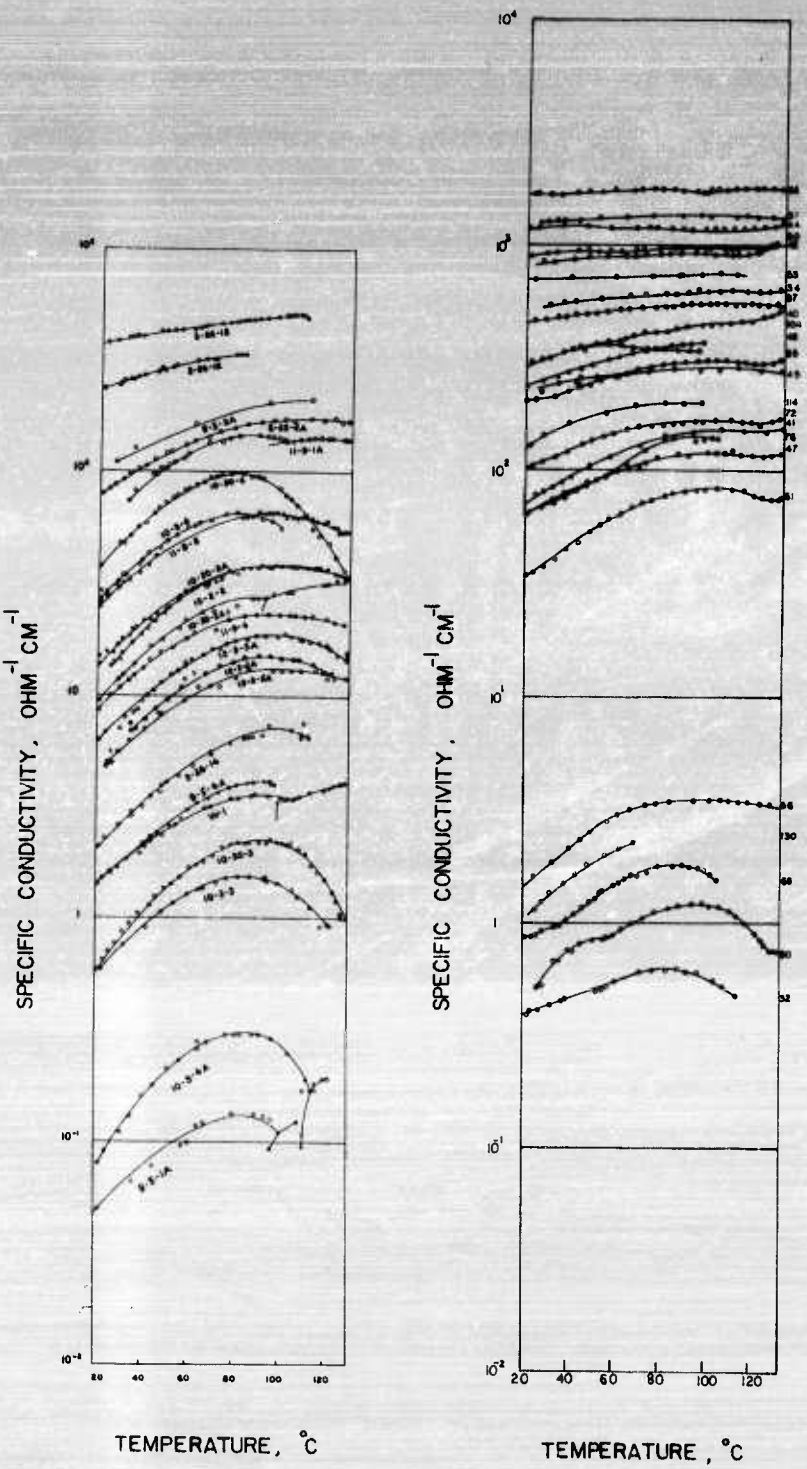

FIGURE 11 - ELECTRICAL CONDUCTIVITY DATA FROM 20° TO 133° C

THE RECENT DATA IS DISPLAYED ON THE RIGHT. EARLIER DATA IS ON THE LEFT.

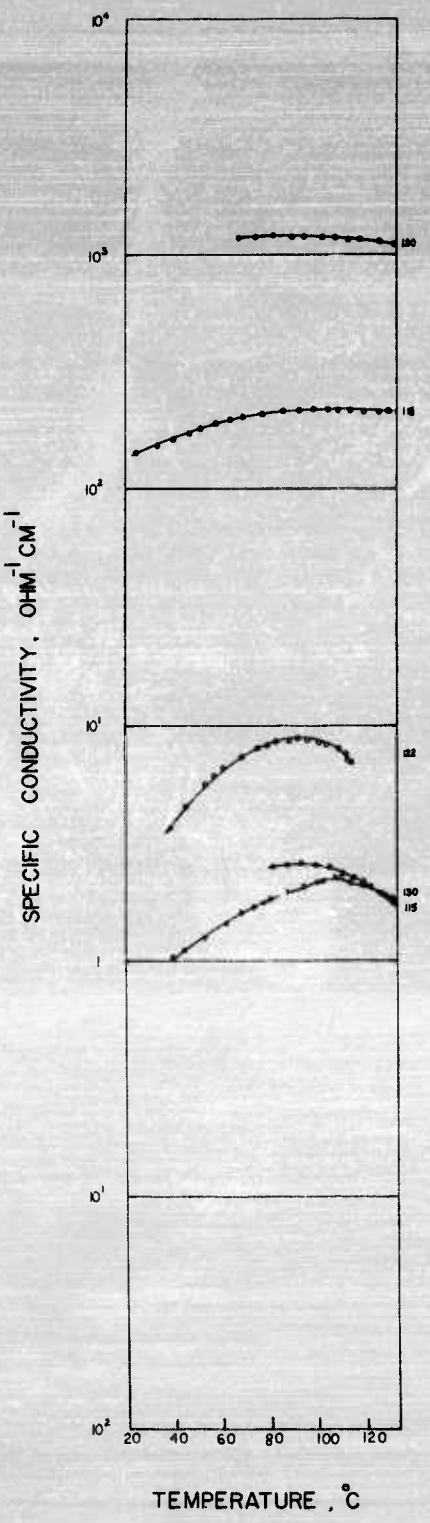

FIGURE 12 - CONDUCTIVITY DATA AT CONSTANT PRESSURE.

REFERENCES

1. Progress Report of December 9, 1963.
2. K. Lark-Horovitz and V. A. Johnson, Methods of Experimental Physics, Volume 6, Part B, Academic Press (1959).
3. I. Isenberg and F. R. Green, Rev. Sci. Instr. 19, 685 (1948).
4. B. R. Russell and C. Wahlig, Rev. Sci. Instr. 21, 1028 (1950).
5. C. A. Kraus, E. S. Carney, and W. C. Johnson, J. Am. Chem. Soc., 49, 2206 (1927).
6. W. C. Johnson and A. W. Meyer, J. Am. Chem. Soc., 54, 3621 (1932).
7. C. A. Kraus, J. Am. Chem. Soc., 30, 653 (1908).
8. P. R. Marshall and M. Hunt, J. Phys. Chem. 60, 732 (1956).
9. I. Warshawsky, J. Inorg. Nucl. Chem. 25, 601 (1963).
10. W. C. Klingelhoefer, Anal. Chem. 34, 1751 (1962).
11. W. H. Kohl, Materials and Techniques for Electron Tubes, Reinhold (1960).
12. L. Holland, The Properties of Glass Surfaces, Wiley (1964).
13. C. A. Kraus, J. Am. Chem. Soc. 43, 749 (1921).
14. C. A. Kraus and W. W. Lucasse, J. Am. Chem. Soc. 43, 2529 (1921).

TABLE I - COMPOSITION OF LOW TEMPERATURE SAMPLES

SAMPLE NO.	MOLE FRACTION OF NA*	SAMPLE NO.	MOLE FRACTION
3-26-18	1.17×10^{-1}	137	1.15×10^{-1}
3-26-10	5.32×10^{-2}	145	1.08×10^{-1}
3-26-15	5.20×10^{-2}	163	1.03×10^{-1}
4-26-8	5.14×10^{-2}	123	7.2×10^{-2}
10-3-1A	5.04×10^{-2}	148	6.0×10^{-2}
3-26-12	4.60×10^{-2}	159	5.55×10^{-2}
33	4.04×10^{-2}	147	5.8×10^{-2}
3-26-9	3.89×10^{-2}	40	5.2×10^{-2}
4-26-2	3.59×10^{-2}	104	4.5×10^{-2}
10-8-4	2.97×10^{-2}	48	4.4×10^{-2}
11-9-1A	2.92×10^{-2}	144	4.5×10^{-2}
28	2.85×10^{-2}	161	3.63×10^{-2}
26	2.81×10^{-2}	114	3.65×10^{-2}
4-26-1	2.47×10^{-2}	114	3.60×10^{-2}
10-30-3A	2.28×10^{-2}	158	3.05×10^{-2}
3-26-16	1.89×10^{-2}	131	2.65×10^{-2}
4-26-7	1.68×10^{-2}	70	2.65×10^{-2}
4-26-5A	1.65×10^{-2}	83	2.08×10^{-2}
4-26-3	1.34×10^{-2}		
29	1.30×10^{-2}		
9-5-4A	1.19×10^{-2}		
3-26-17	1.09×10^{-2}		
10-3-3	6.62×10^{-3}		
X-15	5.48×10^{-3}		
10-8-4A	2.94×10^{-3}		
10-8-3	1.74×10^{-3}		

*Mole fraction of sodium is obtained from the conductivity at $-33.5^{\circ}C$ by reference to Kraus' data[13][14]

TABLE II - COMPOSITION OF HIGH TEMPERATURE SAMPLES

SAMPLE NO.	MOLE FRACTION	SAMPLE NO.	MOLE FRACTION
3-26-15	5.20×10^{-2}	66	9.9×10^{-2}
3-26-12	4.60×10^{-2}	51	8.4×10^{-2}
9-5-3A	3.37×10^{-2}	44	8.21×10^{-2}
8-22-2A	3.22×10^{-2}	50	7.3×10^{-2}
11-9-1A	3.00×10^{-2}	42	7.0×10^{-2}
10-30-4	2.78×10^{-2}	53	6.6×10^{-2}
10-3-4	2.57×10^{-2}	34	5.75×10^{-2}
11-9-3	2.53×10^{-2}	87	5.60×10^{-2}
10-30-3A	2.278×10^{-2}	40	4.95×10^{-2}
10-3-2	2.10×10^{-2}	104	4.85×10^{-2}
10-30-2A	2.01×10^{-2}	48	4.50×10^{-2}
11-9-4	1.97×10^{-2}	85	4.30×10^{-2}
10-3-3A	1.82×10^{-2}	45	4.40×10^{-2}
10-3-2A	1.73×10^{-2}	114	3.60×10^{-2}
10-3-5A	1.70×10^{-2}	72	3.38×10^{-2}
3-26-14	1.35×10^{-2}	41	3.15×10^{-2}
9-5-4A	1.192×10^{-2}	76	3.10×10^{-2}
W-1	1.17×10^{-2}	47	3.10×10^{-2}
10-30-3	7.1×10^{-3}	61	2.70×10^{-2}
10-3-3	6.95×10^{-3}	56	1.16×10^{-2}
10-3-4A	3.50×10^{-3}	130	9.6×10^{-3}
9-5-1A	2.40×10^{-3}	68	9.0×10^{-3}
		80	6.5×10^{-3}
		32	5.7×10^{-3}

TABLE IIA - COMPOSITION OF SAMPLES AT CONSTANT PRESSURE

SAMPLE	MOLE FRACTION	PRESSURE, ATM.
120	8.0×10^{-2}	200
116	3.7×10^{-2}	200
122	1.34×10^{-2}	120
130	9.6×10^{-3}	200
115	8.4×10^{-3}	200

TABLE III - EFFECTIVENESS OF CLEANING PROCEDURES

WASH	RINSE	MOLECULES $\frac{H_2O}{SQ\ \mathring{A}}$ NO BAKE	BAKE◇
HF	H_2O	*≠64	--
None	None	≠59	≠≠78
HNO_3	H_2O	≠24	--
Acetone	None	≠≠22	≠≠12
HNO_3	H_2O, Acetone	≠≠20	≠≠11
Soap	H_2O	≠17	--
		≠16	--
HNO_3	H_2O, NH_4OH	≠≠14	≠≠ 4.4
HNO_3	H_2O	≠≠11	--
Cold Aqua Regia	H_2O	≠≠ 7	≠≠ 7
Hot Soap	Hot H_2O	≠≠ 5.2	≠≠ 4.2
Hot Aqua Regia	Hot H_2O	≠≠ 2.9	≠≠ 3.2
		≠≠ 6.0	
Chromic Acid	H_2O	≠≠ 3.2	≠≠ 4.1
Glacial Acetic Acid	Hot H_2O	≠≠ 2.8	--
HF, HNO_3, Soap, H_2O	H_2O	≠≠ 2.2	≠≠ 2.2

◇Bakeout 2 hours 400°C plus 1 hour 200°C

*Reacted 20 minutes, all others 15 minutes

≠Run No. 1

≠≠Run No. 2

£Vac - NH_3

Contract NONR 3437(00)

Distribution List for Semiannual and Final Technical Summary Reports

Agency	No. of Copies
Director, Advanced Research Projects Agency The Pentagon Washington, 25, D.C.	6
Chief of Naval Research Department of the Navy Washington, 25, D.C. Attn: Code 429	2
Commanding Officer Office of Naval Research Branch Office 1030 East Green Street Pasadena, 1, California	1
Chief, Bureau of Naval Weapons Department of the Navy Washington, 25, D.C.	
Attn: RRRE-6	1
RAPP-33	1
RAAE-511	1
DLI-3	1
Space Sciences Laboratory Litton Systems, Inc. Beverly Hills, California	1
AVCO-Everett Research Laboratory Everett, Massachusetts	1
Plasma Propulsion Laboratory Republic Aviation Corporation Farmingdale, New York	1
Stevens Institute of Technology Hoboken, New Jersey Attn: Winston H. Bostick	1
Astro Electronics Division RCA Laboratories Radio Corporation of America Princeton, New Jersey	1

Agency	No. of Copies
Allison Division General Motors Corporation Indianapolis, Indiana	1
Research Laboratories United Aircraft Corporation East Hartford, 8, Connecticut	1
Cambridge Research Laboratory L.G. Hanscom Field Bedford, Massachusetts	1
Electro-Optical Systems, Inc. 125 North Vinedo Avenue Pasadena, California	1
Space Sciences Laboratory Missile and Space Vehicle Dept. General Electric Company Philadelphia, 24, Pennsylvania	1
Geophysics Research and Development Center University of Maryland College Park, Maryland	1
Plasma Flow Section NASA, Lewis Research Center Cleveland, 35, Ohio	1
Experimental Physics Dept. Aeronutronics Ford Motor Company Newport Beach, California	1
California Institute of Technology 1201 East California Street Pasadena, California Attn: Robert G. Jahn	1
Plasmadyne Corporation Santa Ana, California	1
The Pennsylvania State University University Park, Pennsylvania Attn: Dr. H. Li	1
Gas Dynamic Laboratory Northwestern University Evanston, Illinois Attn: Dr. Ali Cambel	1

Agency	No. of Copies
Physics and Adv ced Systems Dept. Reaction Motors Division Thiokol Chemical Corporation Denville, New Jersey	1
Atlantic Research Corporation Alexandria, Virginia	1
Armed Services Technical Information Agency Arlington Hall Station Arlington, 12, Virginia	10
Office of Technical Services Department of Commerce Washington, 25, D.C.	1
Professor E. Charles Evers Associate Professor of Chemistry University of Pennsylvania Philadelphia, Pennsylvania	1
Hughes Research Laboratories 3011 Malibu Canyon Road Malibu, California Attn: Dr. R. C. Knechtli	1
Rocket Power-Telco 3016 East Foothill Boulevard Pasadena, California Attn: Mr. M. Farber	1
Cambridge Research Laboratories Bedford, Massachusetts Attn: Code CKZAP, Dr. Norman Rosenberg	1
ASRMPE-1 Aeronautical Systems Division Air Force Systems Command Wright-Patterson Air Force Base, Ohio Attn: K. E. Vickers, or 2nd Lt Carl N. Caputo	1
Professor J. C. Thompson University of Texas Austin, 12, Texas	1
Chief, Library NASA-Lewis Research Center 21000 Brookpark Road Cleveland, Ohio 44135	1

Agency	No. of Copies
Mr. Jack A. Myers Westinghouse Electric Corporation P. O. Box 746 Baltimore, 3, Maryland	1
Dr. R. C. Himes, Chief Physical Chemical Research Battelle Memorial Institute 505 King Avenue Columbus, Ohio 43201	1

UNCLASSIFIED